Exchange and the Dielectric Screening Function*

LEONARD KLEINMAN
Department of Physics, University of Texas, Austin, Texas 78712
(Received 15 November 1967; revised manuscript received 12 April 1968)

Using many-body techniques, we evaluate the three dielectric screening functions of a free-electron gas including exchange self-energy and exchange ladder bubble diagrams. The three dielectric functions are $\epsilon_{kt}(\kappa, \omega)$, $\epsilon_{tt}(\kappa, \omega)$, and ϵ_{kk}, (κ, ω), appropriate for screening the interaction between an electron and a test charge, between a pair of test charges, and between a pair of electrons. An approximation for integrals of the screened exchange interaction previously used by Hubbard and by us enables us to evaluate the dielectric screening functions for all values of wave vector κ and frequency ω. The form of ϵ_{kt} and ϵ_{tt} is similar but not identical to that obtained previously using self-consistent-field techniques.

I. INTRODUCTION

EVER since Lindhard[1] derived the dielectric screening function in the random-phase approximation (RPA), there has been much effort expended toward obtaining the dielectric function in approximations beyond the RPA. In spite of this fact, no one has included exchange effects in calculating something as simple as the lifetime of an electron above the Fermi surface of a metal [which depends only on an integral of $\mathrm{Im}1/\epsilon(\kappa, \omega)$]. The reason for this is that the extreme difficulty of carrying the dielectric function beyond the RPA has forced most workers to work in limits which have no applicability to the electron lifetime problem. DuBois[2] has calculated the contributions of the diagrams shown in Figs. 1(a) and 1(b) (with a bare Coulomb interaction) to $\epsilon(\kappa, \omega)$ in the limit $\kappa \to 0$. Osaka[3] calculated the contributions of all iterations of diagrams in 1(a) and 1(b); a typical such diagram being shown in 1(c). He used a Coulomb interaction screened with a static RPA dielectric constant and worked in the limit $\omega = 0$, $\kappa \to 0$. Glick[4] used a Thomas-Fermi screened interaction in summing the same diagrams as Osaka but was able to work in the somewhat more general limit $\kappa \to 0$, $\omega \to 0$, but the ratio $r = \kappa/\omega$ a free variable. Geldart and Vosko[5] obtained $\Pi = \kappa^2(\epsilon - 1)$ including diagrams of the form 1(a), 1(b), and 1(d). They used the full frequency-dependent RPA screened Coulomb interaction but were only able to obtain results in the $r = 0$ and $r = \infty$ limits. They showed that in order to satisfy their compressibility theorem

$$C/C_0 = \Pi^\infty/\Pi_0^\infty \tag{1}$$

to order r_s^2 in the high-density limit, one must include the diagram 1(d). In Eq. (1), C is the compressibility calculated from the Gell-Mann and Brueckner[6] result for the correlation energy at high density, Π^∞ is the $r = \infty$ limit of Π, and the subscript zero signifies the RPA value. On the other hand, Glick[4] has demonstrated that unless the complete set of ladder bubble diagrams are summed (which Geldart and Vosko did not do) the dielectric function will have an unphysical singularity for $r = (2k_F)^{-1}$.

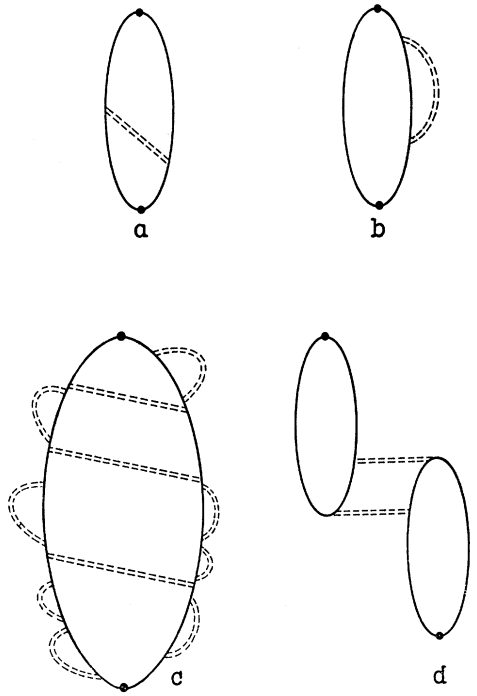

FIG. 1. Diagrams included by various authors in calculating the dielectric constant. The doubly dashed line represents the Coulomb interaction screened in the RPA or some approximation of the RPA.

Hubbard[7] has suggested an approximation for the sum of the ladder bubble diagrams which allows one to

* Research sponsored by the U. S. Air Force Office of Scientific Research Office of Aerospace Research, under Grant No. AFOSR 68-1507.

[1] J. Linhard, Kgl. Danske Videnskab. Selskab, Mat. Fys. Medd. **28**, 8 (1954).
[2] D. F. DuBois, Ann. Phys. (N.Y.) **7**, 174 (1959), Appendix A.
[3] Y. Osaka, J. Phys. Soc. Japan **17**, 547 (1962).
[4] A. J. Glick, Phys. Rev. **129**, 1399 (1963).
[5] D. J. W. Geldart and S. H. Vosko, Can. J. Phys. **44**, 2137 (1966).
[6] M. Gell-Mann and K. A. Brueckner, Phys. Rev. **106**, 364 (1957).
[7] J. Hubbard, Proc. Roy. Soc. (London) **A243**, 336 (1957).

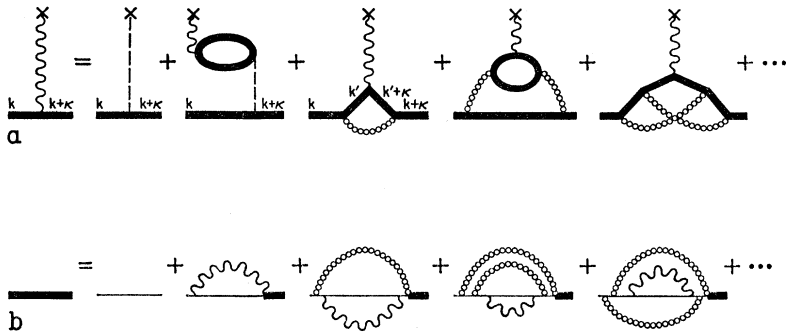

FIG. 2. Diagrammatic coupled integral equations for ϵ_{kt} and ϵ_{et}. The wiggly and bubbly lines represent the Coulomb interaction screened by ϵ_{kt} and $\epsilon_{kk'}$, respectively.

estimate corrections to the dielectric function for all values of κ and ω. Unfortunately, he made a computational error; he also neglected to include the exchange self-energy correction, without whose inclusion the ladder bubble diagrams yield an incorrect plasma frequency. We[8] have recently, using self-consistent-field (SCF) techniques, evaluated the dielectric function including screened exchange matrix elements and the exchange self-energy. Our calculation corresponds as closely as possible (in the SCF theory) to summing the same set of diagrams as Glick[4] and Osaka,[3] but we used the approximation of Hubbard so as to obtain ϵ for all values of κ and ω. Our dielectric constant was correct in every limit in which we could test it except that it did not obey the compressibility theorem.

In this paper we develop a simplified method for summing the same set of diagrams as Glick[4] and Osaka,[3] and again we use the Hubbard approximation so as to obtain the dielectric function for all values of κ and ω. Besides obtaining the ordinary dielectric function, which we call ϵ_{tt} because it screens the potential seen by one test charge due to another, we also obtain ϵ_{kt} and $\epsilon_{kk'}$, which screen the potential seen by the kth electron due to a test charge and due to the k'th electron. The functions ϵ_{tt} and ϵ_{kt} are similar but not identical to those we obtained using SCF techniques.[8] We are not able to say which result is more nearly correct; however, the diagrammatic method has the advantage that higher-order diagrams may be included and, in principle at least, the dielectric function calculated to as great an accuracy as one wishes. The diagrams also yield $\epsilon_{kk'}$, which we were unable to obtain with the SCF technique. The main advantage of the diagrams is, however, that they demonstrate clearly what are the correct dielectric screening functions to use in calculating an electron's self-energy (and hence its lifetime).

II. DIELECTRIC SCREENING FUNCTIONS

In Fig. 2 we show the diagrammatic coupled integral equations for ϵ_{et}, where ϵ_{et} is the test-charge–electron dielectric function ϵ_{kt} averaged over all $\mathbf{k}<k_F$. The dashed line represents the bare Coulomb interaction; the wiggly line represents the Coulomb interaction screened by ϵ_{kt}, i.e., it includes all vertex corrections at one end of the Coulomb line; the bubbly line represents the Coulomb interaction screened by $\epsilon_{kk'}$, i.e., it includes all vertex corrections at both ends of the Coulomb line. Note that the interaction of an electron with another electron or with itself, providing there is an intervening vertex, is screened by $\epsilon_{kk'}$, but that a self-interaction with no intervening vertex is screened by ϵ_{kt}. This is demonstrated clearly in Fig. 3, where the simplest self-energy diagram of Fig. 2(b) is expanded into an infinite hierarchy of diagrams. Diagram (a) is equal to (b) (the double dashed line represents a Coulomb interaction screened by ϵ_{tt}, i.e., with no vertex corrections) plus diagrams (c), (d), (e), $\cdots$, identical with (b) but for single, double, triple, $\cdots$ vertex corrections at one end only. These vertex corrections are Coulomb lines screened by $\epsilon_{kk'}$, and so they themselves contain vertex corrections at both ends. Diagrams (g), (h), and (v) are just (c), (d), and (e) with no further vertex corrections; (i) and (j) come from (c) with a single vertex correction to the vertex correction; (k), (l), (m), and (n) come from (d) with a single vertex correction to one of the vertex corrections; (o), (p), (q), and (r) arise from adding a vertex correction to a vertex correction to the vertex correction of (c); (s), (t), and (u) arise from adding a double vertex correction to one end of the vertex correction of (c) or adding a single one to each end. Note that had diagram (a) contained a bubbly instead of a wiggly Coulomb line, we should have had to add vertex corrections on both ends of (b). The diagram like (g) but with the vertex correction on the other end would have been identical to (g), the diagram like (g) but with vertex corrections on both ends would have been identical to (j); in fact, every diagram would have appeared twice.

We now solve the integral equations of Fig. 2 for ϵ_{et}, keeping the first three terms on the right of 2(a) and the first two on the right of 2(b). By iteration one sees that this is sufficient to generate all the diagrams

[8] L. Kleinman, Phys. Rev. **160**, 585 (1967).

of Glick[4] and Osaka,[3] but with the addition of vertex corrections to all the screened interaction lines. In practice we shall approximate all screened interaction lines (except the line to the external vertex) in a sufficiently crude manner that these additional vertex corrections do not enter. Once we have ϵ_{et} we will easily be able to obtain ϵ_{kt}, ϵ_{tt}, and $\epsilon_{kk'}$. In principle, we could then recalculate ϵ_{et} using Coulomb lines screened by the ϵ_{kt} and $\epsilon_{kk'}$ of the previous interaction and thus include the extra vertex corrections. Following the usual rules,[9] we have from Fig. 2(a),

$$\sum_k V_e(\kappa)S(k)S(k+\kappa)=v(\kappa)\sum_k S(k)S(k+\kappa)$$
$$+2iV_e(\kappa)v(\kappa)\sum_{kk'}S(k)S(k+\kappa)S(k')S(k'+\kappa)$$
$$-iV_e(\kappa)\sum_{kk'}S(k')S(k'+\kappa)V_{ee}(k,k',k'+\kappa)$$
$$\times S(k)S(k+\kappa), \quad (2)$$

where $v(\kappa)=8\pi/\kappa^2$ is the Fourier transform of wave vector κ of the potential of an unscreened unit test charge oscillating with frequency $\kappa_0=\omega$; $V_{ee}(k,k',k'')$ is the screened electron–electron interaction (see Fig. 5), and

$$V_e(\kappa)=v(\kappa)/\epsilon_{et}(\kappa,\omega) \quad (3)$$

is the screened test-charge potential seen by an average[10] electron in the Fermi sea. The sum over k stands for

$$(2\pi)^{-4}\int d^3k\,dk_0,$$

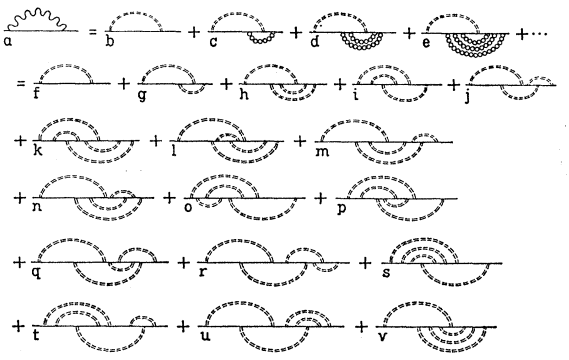

FIG. 3. Infinite set of self-energy diagrams with ordinary ϵ_{tt} screening of Coulomb lines which is generated by a single self-energy diagram with ϵ_{kt} screening.

and $S(k)$ is the electron propagator given by

$$S(k)=f(\mathbf{k})/[k_0-\omega(\mathbf{k})-M(k)-i\eta]$$
$$+[1-f(\mathbf{k})]/[k_0-\omega(\mathbf{k})-M(k)+i\eta], \quad (4)$$

where $M(k)$ is the self-energy to be determined from the equation corresponding to Fig. 2(b), $\omega(\mathbf{k})=k^2$ (in atomic units), η is a positive infinitesimal, and $f(\mathbf{k})$ is the zero-temperature Fermi function. If we approximate M and V_{ee} by the frequency-independent functions $M(\mathbf{k})$ and $V_{ee}(\mathbf{k},\mathbf{k}',\mathbf{k}'+\kappa)$ the integrals over k_0 and k_0' in Eq. (2) become trivial. Solving for $v(\kappa)/V_e(\kappa)$ one obtains

$$\epsilon_{et}(\kappa,\omega)=1+2v(\kappa)(2\pi)^{-3}\int\Theta(k')d^3k'-(2\pi)^{-3}\iint\Theta(k)V_{ee}(\mathbf{k},\mathbf{k}',\mathbf{k}'+\kappa)\Theta(k')d^3k\,d^3k'\Big/\int\Theta(k)d^3k, \quad (5)$$

where

$$\Theta(k)=\frac{f(\mathbf{k})[1-f(\mathbf{k}+\kappa)]}{\omega(\mathbf{k}+\kappa)+M(\mathbf{k}+\kappa)-\omega(\mathbf{k})-M(\mathbf{k})-\omega-i\eta}+\frac{f(\mathbf{k}+\kappa)[1-f(\mathbf{k})]}{\omega(\mathbf{k})+M(k)-\omega(\mathbf{k}+\kappa)-M(\mathbf{k}+\kappa)+\omega-i\eta}. \quad (6)$$

We show in the Appendix that Eq. (6) is equivalent to

$$\Theta(k)=\frac{f(\mathbf{k})-f(\mathbf{k}+\kappa)}{\omega(\mathbf{k}+\kappa)+M(\mathbf{k}+\kappa)-\omega(\mathbf{k})-M(\mathbf{k})-\omega-i\eta\,\mathrm{sgn}\omega} \quad (7)$$

when M is real. When M is complex, one can neglect the infinitesimal η and Eq. (7) follows immediately from Eq. (6). Let us write

$$\Theta(k)=[f(\mathbf{k})-f(\mathbf{k}+\kappa)]D_-^*(k),$$

where

$$D_\pm(k)=[\omega(\mathbf{k}+\kappa)+M(\mathbf{k}+\kappa)-\omega(\mathbf{k})-M(\mathbf{k})\pm\omega+i\eta\,\mathrm{sgn}\omega]^{-1}. \quad (8)$$

[9] J. R. Schrieffer, *Theory of Superconductivity* (W. A. Benjamin, Inc., New York, 1964), Sec. 5–9.
[10] This average is of course defined by $V_e(\kappa)\Sigma_k S(k)S(k+\kappa)=\Sigma_k V_k(\kappa)S(k)S(k+\kappa)$.

Then one easily sees that[11]

$$\int \Theta(k)\,d^3k = \int f(\mathbf{k})[D_+(k)+D_-^*(k)]\,d^3k, \tag{9}$$

$$\iint \Theta(k)\,V_{ee}(\mathbf{k},\mathbf{k}',\mathbf{k}'+\boldsymbol{\kappa})\,\Theta(k')\,d^3k\,d^3k' = \iint f(\mathbf{k})f(\mathbf{k}')\{D_+(k)D_+(k')\,V_{ee}(\mathbf{k},\mathbf{k}',\mathbf{k}'+\boldsymbol{\kappa})$$
$$+D_-^*(k)D_-^*(k')\,V_{ee}(\mathbf{k}+\boldsymbol{\kappa},\mathbf{k}'+\boldsymbol{\kappa},\mathbf{k}')+D_+(k)D_-^*(k')\,V_{ee}(\mathbf{k}+\boldsymbol{\kappa},\mathbf{k}',\mathbf{k}'-\boldsymbol{\kappa})$$
$$+D_-^*(k)D_+(k')\,V_{ee}(\mathbf{k},\mathbf{k}'+\boldsymbol{\kappa},\mathbf{k}')\}\,d^3k\,d^3k'. \tag{10}$$

We now make the approximation[7,8] that $V_{ee}(\mathbf{k},\mathbf{k}',\mathbf{k}'+\boldsymbol{\kappa})$ in the integral of $\mathbf{k}$ and $\mathbf{k}'$ over the Fermi sea takes on the average value

$$V_{ee}(\mathbf{k},\mathbf{k}',\mathbf{k}'+\boldsymbol{\kappa}) = V_{ee}(\mathbf{k}'-\mathbf{k}) \approx 8\pi/(2\alpha k_F^2+K_S^2) \tag{11}$$

and that $V_{ee}(\mathbf{k}'\pm\boldsymbol{\kappa}-\mathbf{k})\approx 8\pi/(2\alpha k_F^2+\kappa^2+K_S^2)$, where K_S is an inverse screening wavelength and α is a factor to be determined in the next section.[12] Defining

$$\chi(\kappa,\pm\omega) = 4(\pi\kappa)^{-2}\int D_\pm(k)f(\mathbf{k})\,d^3k, \tag{12}$$

we have

$$\epsilon_{et}(\kappa,\omega) = 1+\tfrac{1}{2}[\chi(\kappa,+\omega)+\chi^*(\kappa,-\omega)]-\frac{1}{2}\left[\frac{A[\chi^2(\kappa,+\omega)+\chi^{*2}(\kappa,-\omega)]+2B\chi(\kappa,\omega)\chi^*(\kappa,-\omega)}{\chi(\kappa+\omega)+\chi^*(\kappa,-\omega)}\right], \tag{13}$$

where

$$A = \tfrac{1}{2}[\kappa^2/(2\alpha k_F^2+K_S^2)],$$
$$B = \tfrac{1}{2}[\kappa^2/(2\alpha k_F^2+\kappa^2+K_S^2)]. \tag{14}$$

To evaluate $\chi(\kappa,\pm\omega)$ we first must determine $M(\mathbf{k})$. The Dyson equation of Fig. 2(b) is (first two diagrams on right-hand side only)

$$S(k) = S_0(k)+S_0(k)M(k)S(k),$$

where

$$M(k) = i(2\pi)^{-4}\int S_0(k+q)\,V_k(q)\,d^3q\,dq_0$$
$$= -(2\pi)^{-3}\int f(\mathbf{k}+\mathbf{q})\,V_k(\mathbf{q})\,d^3q. \tag{15}$$

Because $M(k)$ is to be integrated over the Fermi sea in Eq. (12) we use the same approximation for $V_k(\mathbf{q}-\mathbf{k})$ as for $V_{ee}(\mathbf{k}'-\mathbf{k})$ [see Eq. (11)]. This is consistent with the fact that to this order neither contains vertex corrections. Thus

$$M(\mathbf{k}) \approx -(2\pi)^{-3}\int f(\mathbf{q})\,V_e(\mathbf{q}-\mathbf{k})\,d^3q$$
$$= -(4/3\pi)[k_F^3/(2\alpha k_F^2+K_S^2)]. \tag{16}$$

Similarly $M(\mathbf{k}+\boldsymbol{\kappa}) = -(4k_F^3/3\pi)(2\alpha k_F^2+\kappa^2+K_S^2)$ and

$$\Delta(\kappa) = M(\mathbf{k}+\boldsymbol{\kappa})-M(\mathbf{k})$$
$$= \frac{4}{3\pi}k_F^3\frac{\kappa^2}{(2\alpha k_F^2+\kappa^2+K_S^2)(2\alpha k_F^2+K_S^2)}. \tag{17}$$

[11] This follows immediately from letting $\mathbf{k}+\boldsymbol{\kappa}\to\mathbf{k}$ in the $f(\mathbf{k}+\boldsymbol{\kappa})$ terms and then letting $\boldsymbol{\kappa}\to-\boldsymbol{\kappa}$.

[12] Previously (Ref. 8), following Hubbard (Ref. 7), we did not have the factor 2α multiplying k_F^2 in the denominator of $V_{ee}(\mathbf{k}'-\mathbf{k}+\boldsymbol{\kappa})$.

The integral (12) for

$$\chi(\kappa,\pm\omega) = \chi_1(\kappa,\pm\omega) - i\,(\mathrm{sgn}\omega)\,\chi_2(\kappa,\pm\omega) \tag{18}$$

yields

$$\chi_1(\kappa,\pm\omega) = \frac{2}{\pi\kappa^3}\left\{\left[k_F^2-\left(\frac{\kappa^2+\Delta(\kappa)\pm\omega}{2\kappa}\right)^2\right]\right.$$
$$\left.\times\ln\left|\frac{\kappa^2+\Delta(\kappa)\pm\omega+2\kappa k_F}{\kappa^2+\Delta(\kappa)\pm\omega-2\kappa k_F}\right| + \frac{k_F}{\kappa}[\kappa^2+\Delta(\kappa)\pm\omega]\right\}, \tag{19}$$

$$\chi_2(\kappa,+\omega) = \frac{2}{\kappa^3}\left[k_F^2-\left(\frac{\kappa^2+\Delta(\kappa)+\omega}{2\kappa}\right)^2\right]$$
$$\text{if}\quad \omega+\Delta(\kappa)<2\kappa k_F-\kappa^2 \tag{20}$$
$$=0 \qquad \text{otherwise},$$

$$\chi_2(\kappa,-\omega) = \frac{2}{\kappa^3}\left[k_F^3-\left(\frac{\kappa^2+\Delta(\kappa)-\omega}{2\kappa}\right)^2\right]$$
$$\text{if}\quad \kappa^2-2k_F<\omega-\Delta(\kappa)<\kappa^2+2k_F\kappa \tag{21}$$
$$=0 \qquad \text{otherwise}.$$

This $\chi(\kappa,\pm\omega)$ is identical to that in the SCF theory[8] except for the $-\ \mathrm{sgn}\omega$ factor multiplying χ_2 in Eq. (18). This factor leads to the field-theoretic ϵ_{tt} obeying the condition[13] $\epsilon_{tt}(\kappa,+\omega)=\epsilon_{tt}(\kappa,-\omega)$, whereas the true (SCF) dielectric constant obeys $\epsilon_{tt}(\kappa,+\omega)=\epsilon_{tt}^*(\kappa,-\omega)$. Note that ϵ_{et} of Eq. (13) also has the property $\epsilon_{et}(\kappa,+\omega)=\epsilon_{et}(\kappa,-\omega)$.

[13] P. Nozieres, *Theory of Interacting Fermi Systems* (W. A. Benjamin, Inc., New York, 1964), Appendix A.

Now that we have $\epsilon_{et}(\kappa, \omega)$, the dielectric constant appropriate to an *average* electron in the Fermi sea, we can easily obtain the dielectric constant appropriate to a particular electron of wave vector $\mathbf{k}$. From Fig. 2(a) we have (dropping the contributions from the incoming and outgoing propagators)

$$V_k(\kappa) = v(\kappa) + 2iv(\kappa) \sum_{k'} V_{k'}(\kappa) S(k') S(k'+\kappa) - i \sum_{k'} V_{k'}(\kappa) V_{ee}(k, k', k'+\kappa) S(k') S(k'+\kappa). \quad (22)$$

Now $V_{k'}(\kappa) = V_{k'-\kappa}(\kappa)$ is the screened potential matrix element between states $|\mathbf{k}'\rangle$ and $|\mathbf{k}'\pm\boldsymbol{\kappa}\rangle$; it is summed in (22) over $\mathbf{k}'$ within the Fermi sea and therefore may be replaced by its average value $V_e(\boldsymbol{\kappa})$. Thus,

$$V_k(\kappa) = v(\kappa) - 2v^2(\kappa)(2\pi)^{-3}[\epsilon_{et}(\boldsymbol{\kappa}, \omega)]^{-1} \times \int \Theta(k') d^3k' + (2\pi)^{-3} v(\kappa)[\epsilon_{et}(\boldsymbol{\kappa}, \omega)]^{-1} \times \int \Theta(k') V_{ee}(\mathbf{k}, \mathbf{k}', \mathbf{k}'+\boldsymbol{\kappa}) d^3k'. \quad (23)$$

Using

$$\int \Theta(k') V_{ee}(\mathbf{k}, \mathbf{k}', \mathbf{k}'+\boldsymbol{\kappa}) d^3k' = \int f(\mathbf{k}')[D_-^*(k') V_{ee}(\mathbf{k}, \mathbf{k}', \mathbf{k}'+\boldsymbol{\kappa}) + D_+(k') V_{ee}(-\mathbf{k}, \mathbf{k}'+\boldsymbol{\kappa}, \mathbf{k}')] d^3k' \quad (24)$$

and approximating $V_{ee}(\mathbf{k}'+\boldsymbol{\kappa}+\mathbf{k})$ when $\mathbf{k}'$ only is integrated over the Fermi sea by

$$V_{ee}(\mathbf{k}'+\boldsymbol{\kappa}+\mathbf{k}) \approx 8\pi/[(\mathbf{k}+\boldsymbol{\kappa})^2 + \alpha k_F^2 + K_S^2], \quad (25)$$

one obtains for $\epsilon_{kt}(\boldsymbol{\kappa}, \omega) = v(\kappa)/V_k(\kappa)$,

$$\epsilon_{kt}(\boldsymbol{\kappa}, \omega) = \frac{\epsilon_{et}(\boldsymbol{\kappa}, \omega)}{\epsilon_{et}(\boldsymbol{\kappa}, \omega) - \frac{1}{2}[\chi(\boldsymbol{\kappa}, +\omega) + \chi^*(\boldsymbol{\kappa}, -\omega)] + \frac{1}{2}[A_{\mathbf{k}}\chi^*(\boldsymbol{\kappa}, -\omega) + B_{\mathbf{k}}\chi(\boldsymbol{\kappa}, \omega)]}, \quad (26)$$

where

$$A_{\mathbf{k}} = \tfrac{1}{2}[\kappa^2/(k^2 + \alpha k_F^2 + K_S^2)], \qquad B_{\mathbf{k}} = \tfrac{1}{2}\{\kappa^2/[(\mathbf{k}+\boldsymbol{\kappa})^2 + \alpha k_F^2 + K_S^2]\}. \quad (27)$$

To obtain $\epsilon_{tt}(\boldsymbol{\kappa}, \omega)$, the dielectric function with no vertex corrections (this is the "standard" dielectric function), we refer to Fig. 4. Taking diagram (a) = (b) + (c), we have

$$\sum_k V_e(\kappa) S(k) S(k+\kappa) = \sum_k V_t(\kappa) S(k) S(k+\kappa) - i \sum_{kk'} V_e(\kappa) V_{ee}(\mathbf{k}, \mathbf{k}', \mathbf{k}'+\boldsymbol{\kappa}) S(k) S(k+\kappa) S(k') S(k'+\kappa) \quad (28)$$

or

$$\epsilon_{et}^{-1}(\boldsymbol{\kappa}, \omega) = \epsilon_{tt}^{-1}(\boldsymbol{\kappa}, \omega) - i\epsilon_{et}^{-1}(\boldsymbol{\kappa}, \omega) \sum_{kk'} V_{ee}(\mathbf{k}, \mathbf{k}', \mathbf{k}'+\boldsymbol{\kappa}) S(k) S(k+\kappa) S(k') S(k'+\kappa) / \sum_k S(k) S(k+\kappa). \quad (29)$$

The sums in (29) have previously been evaluated in determining ϵ_{et} and thus we obtain

$$[\epsilon_{et}(\boldsymbol{\kappa}, \omega)]^{-1} \left\{1 - \frac{1}{2} \frac{A[\chi^2(\boldsymbol{\kappa}, +\omega) + \chi^{*2}(\boldsymbol{\kappa}, -\omega)] + 2B\chi(\boldsymbol{\kappa}, +\omega)\chi^*(\boldsymbol{\kappa}, -\omega)}{\chi(\boldsymbol{\kappa}, +\omega) + \chi^*(\boldsymbol{\kappa}, -\omega)}\right\} = [\epsilon_{tt}(\boldsymbol{\kappa}, \omega)]^{-1} \quad (30)$$

or

$$\epsilon_{tt}(\boldsymbol{\kappa}, \omega) = 1 + \tfrac{1}{2}[\chi(\boldsymbol{\kappa}, +\omega) + \chi^*(\boldsymbol{\kappa}, -\omega)] \left\{1 - \frac{1}{2} \frac{A[\chi^2(\boldsymbol{\kappa}+\omega) + \chi^{*2}(\boldsymbol{\kappa}, -\omega)] + 2B\chi(\boldsymbol{\kappa}, \omega)\chi^*(\boldsymbol{\kappa}, -\omega)}{\chi(\boldsymbol{\kappa}, +\omega) + \chi^*(\boldsymbol{\kappa}, -\omega)}\right\}^{-1}. \quad (31)$$

To obtain $\epsilon_{kk''}(\boldsymbol{\kappa}, \omega)$ we again refer to Fig. 4. We see that diagram (a) = (f) + (g) + (h) + $\cdots$ can be written in the form (dropping incoming and outgoing electron propagators)

$$V_k(\kappa) = V_t(\kappa)\{1 - F(k, k+\kappa)\}. \quad (32)$$

On the other hand, referring to Fig. 5, we see that

$$V_{ee}(k, k', k'') = V_t(\kappa)\{1 - F(k, k+\kappa)\}\{1 - F(k'', k''-\kappa)\}. \quad (33)$$

Replacing the various V's by the bare potential screened by the appropriate dielectric constant and solving (32) and (33) for $\epsilon_{kk''}(\boldsymbol{\kappa}, \omega)$, one finds immediately

$$\epsilon_{kk''}(\boldsymbol{\kappa}, \omega) = \epsilon_{kt}(\boldsymbol{\kappa}, \omega)\epsilon_{k''t}(-\boldsymbol{\kappa}, -\omega)/\epsilon_{tt}(\boldsymbol{\kappa}, \omega). \quad (34)$$

In the present degree of approximation we have shown, and although we have not proven it, it seems likely to be true in general, that $\epsilon_{kt}(\boldsymbol{\kappa}, \omega) = \epsilon_{kt}(\boldsymbol{\kappa}, -\omega)$. Thus,

$$\epsilon_{kk''}(\boldsymbol{\kappa}, \omega) = \epsilon_{kt}(\boldsymbol{\kappa}, \omega)\epsilon_{k''t}(-\boldsymbol{\kappa}, \omega)/\epsilon_{tt}(\boldsymbol{\kappa}, \omega). \quad (35)$$

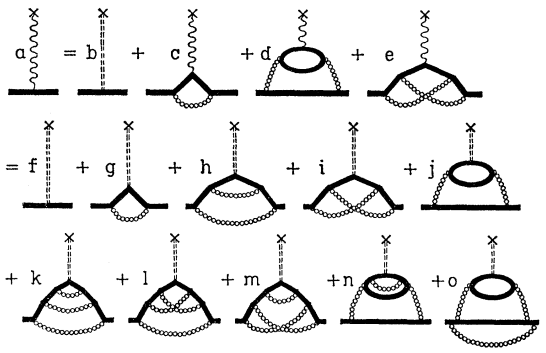

FIG. 4. Diagrammatic integral equation for ϵ_{kl} in terms of ϵ_{tt} and iteration of that equation.

From (26) and (27) we note that $\epsilon_{kl}(\kappa, \omega)$ depends on $\mathbf{k}+\boldsymbol{\kappa}$; hence the minus sign may not be dropped from the κ in (35).

III. DISCUSSION

If we take $K_S^2=\beta k_F$ (the Fermi-Thomas value of β is $4/\pi$) we may evaluate the ratio of $\epsilon_{tt}-1$ to the RPA value in the limit $\omega=0$, $\kappa\to 0$, $k_F\to\infty$. We obtain

$$L=1-\alpha\lambda+\tfrac{1}{2}\beta\pi\lambda^2, \tag{36}$$

where $\lambda=(\pi k_F)^{-1}$. This is to be compared with the value found by Geldart and Vosko[5] from the compressibility:

$$L=1-\lambda-(1-\ln 2)\lambda^2. \tag{37}$$

This implies that in this limit a good choice for the factor α appearing in (11) would be $\alpha=1$. This is not too surprising since for $\kappa\to 0$ only electrons at the Fermi surface contribute to the dielectric screening and the average value of $(\mathbf{k}-\mathbf{k}')^2$ when both are confined to the Fermi surface is $2k_F^2$. On the other hand, for large κ, all $\mathbf{k}$ and $\mathbf{k}'$ contribute equally and the average value of $(\mathbf{k}-\mathbf{k}')^2$ over the entire Fermi sea is $6k_F^2/5$. We would therefore suggest that α be taken as a function of κ, decreasing from its value 1 at $\kappa=0$ to $\frac{3}{5}$ at $\kappa\gg k_F$. The preceding considerations follow from the factor $f(\mathbf{k})-f(\mathbf{k}+\boldsymbol{\kappa})$ in (7) and hence apply to the $V_{ee}(\mathbf{k}-\mathbf{k}')$ and $V_{ee}(\mathbf{k}+\boldsymbol{\kappa}-\mathbf{k}')$ terms together, i.e., the same value of α is used in A and B [Eq. (14)] even though A does not contain κ in its denominator. Similar considerations show that the α in A_k and B_k [Eq. (27)] are identical to those in A and B.

A good estimate of K_S^2 is to be obtained from

$$K^2\epsilon_{\mathrm{RPA}}(K)=K^2+K_S^2, \tag{38}$$

where K is the average momentum transfer, $(2\alpha)^{1/2}k_F$, $(2\alpha k_F^2+\kappa^2)^{1/2}$, $(\alpha k_F^2+k^2)^{1/2}$, and $(\alpha k_F^2+k^2+\kappa^2)$ in A, B, A_k, and B_k, respectively. One finds for $K=\sqrt{2}k_F$ that $K_S^2=1.03k_F$ (cf. the Thomas-Fermi $K_S^2=4k_F/\pi$).[14] Note that the compressibility theorem cannot be satisfied to order λ^2 except with a negative screening constant. Since (37) is valid only in the high-density limit where λ^2 is small, this should not bother us too much. Our choice for K_S^2 is probably as good as one can do over the entire range of the variables ω, κ, and k_F.

The present results differ from the SCF results.[8,15] It appears that these differences are mainly due to a loss of Hermiticity of the potential in Ref. 8 which occured when making the approximation $(\mathbf{k}-\mathbf{k}')^2\to k_F^2$ and $(\mathbf{k}-\mathbf{k}'+\boldsymbol{\kappa})^2\to k_F^2+\kappa^2$. This has been pointed out by Langreth (to be published) along with a prescription for obtaining a Hermitian self-consistent potential. In any event, in those limits in which χ is real, the SCF and field theoretic results are identical. In the limits $\kappa=0$ and $\kappa\to\infty$ one finds χ and hence ϵ_{et} to be real; the field-theoretic and SCF ϵ_{et} are found to be exactly identical in these limits. Equation (30) for $1/\epsilon_{tt}$ is easily seen to be equivalent to Eq. (26) of Ref. 8 whenever ϵ_{et} is real; thus the SCF and field-theoretic ϵ_{ii} are identical when their ϵ_{et} are. The evaluation of the dielectric constants in these limits has been performed in Ref. 8 and will not be repeated here.

In order to improve upon the present calculation, one must both include more diagrams from Figs. 2(a) and 2(b) in the integral equations and screen the

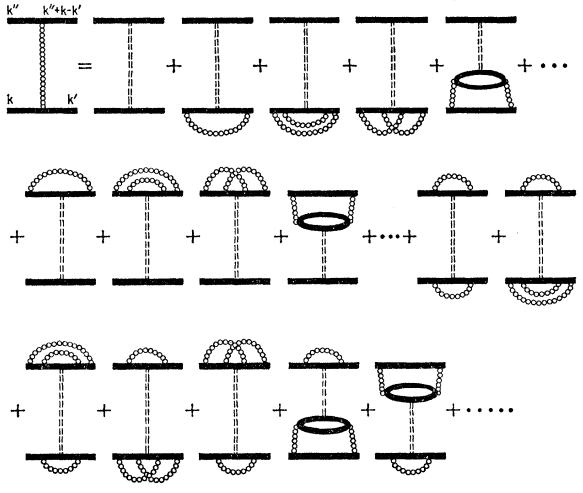

FIG. 5. Diagrammatic equation for $\epsilon_{kk'}$ in terms of ϵ_{tt}.

[14] If one wishes to use only one value of K_S^2 for all momentum transfers, $K_S^2=1.03k_F$ would be a good choice since for large κ the momentum transfer in B is greater than $\sqrt{2}k_F$ and in A is less than $\sqrt{2}k_F$.

[15] This difference holds for positive frequency, i.e., it is not just the trivial one $\epsilon(\kappa,-\omega)=\epsilon(\kappa,\omega)$ versus $\epsilon(\kappa,-\omega)=\epsilon^*(\kappa,\omega)$.

Coulomb lines with the $\epsilon_{kt}(\kappa, \omega)$ and $\epsilon_{kk'}(\kappa, \omega)$ found in this calculation. The inclusion of the fourth diagram on the right-hand side of Fig. 2(a), which when iterated contains Fig. 1(d) among its infinity of diagrams, is needed to satisfy the compressibility theorem to order λ^2. There is no reason for believing, however, that this diagram is any more important than the fifth one, which is of the same order. Although the above program is too complicated to consider attempting, the calculation of Γ, the imaginary part of the self-energy M, is practical and will be the subject of a later paper.[16] We have, from Eq. (15),

$$\Gamma(k) = \mathrm{Im} i(2\pi)^{-4} \int d^4q S_0(k+q) v(\mathbf{q})/\epsilon_{kt}(\mathbf{q}, q_0). \quad (39)$$

Using the fact that $1/\epsilon_{kt}(\mathbf{q}, q_0)$ is analytic above the real axis for positive q_0 and below the real axis for negative q_0, one obtains

$$\Gamma(k) = \pi^{-2} \mathrm{Im} \int d^3q\, (\mathbf{q}-\mathbf{k})^{-2} \{[1-f(\mathbf{q})]\theta[k_0-\omega(\mathbf{q})] - f(\mathbf{q})\theta[\omega(\mathbf{q})-k_0]\}/\epsilon_{kt}[\mathbf{q}-\mathbf{k}, \omega(\mathbf{q})-k_0], \quad (40)$$

where θ is the unit step function. If, as is usually the case, one is interested in the self-energy of an electron on the energy shell, one has $k_0=\omega(\mathbf{k})$. Note from Eqs. (31) and (13) that the effect of exchange is generally to increase ϵ_{tt} and decrease ϵ_{kt}. Hence, if one attempts to improve the self-energy by including exchange effects in ϵ_{tt}, he actually obtains a result less accurate than that of the RPA unless at the same time he also includes the contribution of the infinity of vertex correction diagrams displayed in Fig. 3. Thus we demonstrate the usefulness of ϵ_{kt}, which, without being any more complicated than ϵ_{tt}, automatically includes this infinity of vertex corrections.

Perhaps the largest errors in our dielectric screening functions are due to the use of static vertex corrections. Had we treated everything dynamically [i.e., not dropped the k_0 dependence of $M(k)$ and $V_{ee}(k, k', k'+\kappa)$], we would have found effective-mass corrections from the ω dependence of $\Delta(\kappa)$ of Eq. (17) and renormalization corrections due to the residues of the integration over k_0 and k_0' in Eq. (2). Heine, Nozieres, and Wilkins (HNW)[17] have studied the dielectric constant of a quasiparticle $\epsilon_{k_F}(\kappa, 0)$, where $|\mathbf{k}_F+\boldsymbol{\kappa}| = k_F$. Our dielectric screening function in this limit appears to be equivalent to theirs. They find $\epsilon_{k_F}(\kappa, 0)$ in terms of a vertex function and renormalization factor. In the limit $\kappa \to 0$, the renormalization factor is canceled by one contained in the vertex function and $\epsilon_{k_F}(\kappa \to 0, 0)$ approaches the RPA result but with m^* replacing m. Our static approximation also yields the RPA result in this limit but without the m^* correction. For the denser metals ($2<r_s<3$) m^* is within 2% of m so this correction is small. On the other hand, the cancellation does not occur for larger κ; since the renormalization factor z is believed to be about 0.7 for these metallic densities,[18] errors of this magnitude could be present in our dielectric function. We note, however, that the numerical values of z were obtained[18] using the Hubbard approximation and could conceivably be much closer to unity. Although our $\epsilon_k(\kappa, \omega)$ appears to be equivalent to that of HNW, our electron–electron screening functions are not. Theirs refers to the full four-point vertex function, whereas ours merely screens a single Coulomb interaction line. The relationship between the four-point vertex function and the screened electron–electron interaction is shown graphically[19] in Fig. 6.

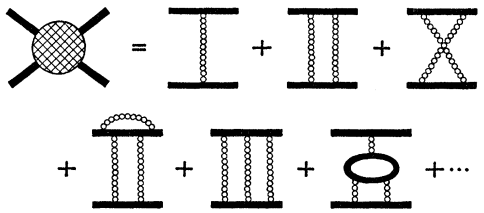

FIG. 6. Relationship between the four-point vertex function and the $\epsilon_{kk'}$ screened Coulomb interaction.

The Hubbard[7] approximation has been widely used because it is the only one that gives the dielectric screening function for all values of wave number and frequency.[20] In this paper we have corrected Hubbard's error of double counting the $(\mathbf{k}-\mathbf{k}'+\boldsymbol{\kappa})$ momentum transfer while neglecting the $(\mathbf{k}-\mathbf{k}')$ momentum transfer altogether. We have also included the self-energy corrections which Hubbard neglected. As we have thoroughly discussed, there are still grave uncertainties in the approximation; it is our feeling, however, that the SCF method, to which the present approximation is equivalent, is inherently more accurate than these uncertainties would indicate. The cancellation of the renormalization factors in the $\omega=0$, $\kappa \to 0$ limit and the fact that the exact plasma frequency is obtained[8] indicate that this may be the case.

---

[16] F. Vernon and L. Kleinman (to be published).

[17] V. Heine, P. Nozieres, and J. W. Wilkins, Phil. Mag. **13**, 741 (1966).

[18] T. M. Rice, Ann. Phys. (N.Y.) **31**, 100 (1965).

[19] The relationship between the four-point vertex function and the Landau quasiparticle interaction function $f(\mathbf{k}, \mathbf{k}')$ is given in Eq. (6-246) of Ref. 13.

[20] The HNW screening function (Ref. 17) is written in terms of undetermined vertex functions and renormalization factors. Only in the $\omega=0$, $\kappa \to 0$ limit is a numerical value obtainable.

ACKNOWLEDGMENT

The author is deeply indebted to Dr. D. F. DuBois for an illuminating discussion of diagrammatic techniques.

APPENDIX

We here show that the $\Theta(k)$ of (7) is identical to that defined in (6). To save writing let $W(\mathbf{k})=\omega(\mathbf{k})+M(\mathbf{k})$. Using

$$(x-a\pm i\eta)^{-1}=P(x-a)^{-1}\mp i\pi\delta(x-a), \quad \text{(A1)}$$

we have immediately from (6) that

$$\mathrm{Re}\Theta(k)=P\frac{f(\mathbf{k})-f(\mathbf{k}+\boldsymbol{\kappa})}{W(\mathbf{k}+\boldsymbol{\kappa})-W(\mathbf{k})-\omega}, \quad \text{(A2)}$$

$$\mathrm{Im}\Theta(k)=i\pi[f(\mathbf{k})+f(\mathbf{k}+\boldsymbol{\kappa})-2f(\mathbf{k})f(\mathbf{k}+\boldsymbol{\kappa})]\times\delta[W(\mathbf{k})-W(\mathbf{k}+\boldsymbol{\kappa})+\omega]. \quad \text{(A3)}$$

Because $f(\mathbf{k})$ is either 0 or 1, $f(\mathbf{k})=f^2(\mathbf{k})$, and thus

$$[f(\mathbf{k})+f(\mathbf{k}+\boldsymbol{\kappa})-2f(\mathbf{k})f(\mathbf{k}+\boldsymbol{\kappa})]=[f(\mathbf{k})-f(\mathbf{k}+\boldsymbol{\kappa})]^2=\pm[f(\mathbf{k})-f(\mathbf{k}+\boldsymbol{\kappa})]. \quad \text{(A4)}$$

If $\mathbf{k}$ and $\mathbf{k}+\boldsymbol{\kappa}$ are both greater or less than k_F, $[f(\mathbf{k})-f(\mathbf{k}+\boldsymbol{\kappa})]=0$ and the $\pm$ sign is immaterial. If, however, $\mathbf{k}>k_F$ and $\mathbf{k}+\boldsymbol{\kappa}<k_F$, the minus sign holds and if $\mathbf{k}<k_F$ and $\mathbf{k}+\boldsymbol{\kappa}>k_F$, the plus sign holds. In the first case $\omega=W(\mathbf{k}+\boldsymbol{\kappa})-W(\mathbf{k})$ is negative and in the second, positive. Thus,

$$\mathrm{Im}\Theta(k)=i\pi\,\mathrm{sgn}\omega[f(\mathbf{k})-f(\mathbf{k}+\boldsymbol{\kappa})]\times\delta[W(\mathbf{k})-W(\mathbf{k}+\boldsymbol{\kappa})+\omega]. \quad \text{(A5)}$$

(A2) and (A5) combine, using (A1), to yield

$$\Theta(k)=\frac{f(\mathbf{k})-f(\mathbf{k}+\boldsymbol{\kappa})}{W(\mathbf{k}+\boldsymbol{\kappa})-W(\mathbf{k})-\omega-i\eta\,\mathrm{sgn}\omega}. \quad \text{(A6)}$$

PHYSICAL REVIEW VOLUME 172, NUMBER 2 10 AUGUST 1968

Specific Heat of a Spherical Type-II Superconductor*

PAUL ZOLLER AND J. R. DILLINGER

Department of Physics, University of Wisconsin, Madison, Wisconsin

(Received 4 December 1967)

Specific-heat measurements on a spherical 7.05 wt% Pb–In alloy [type-II superconductor with $\kappa(T_c)=0.72$] are discussed, with special emphasis on the difference in the effect of irreversibility on the determination of Maki's parameters κ_1 and κ_2 in calorimetric and magnetization measurements. Evidence is presented to show that κ_1 can be extracted reliably from specific-heat measurements even in the presence of severe irreversibility. $\kappa_1(T)/\kappa_1(T_c)$ showed a much stronger temperature dependence than that predicted by current theories for the case of noninfinite mean free path of the electrons.

THE specific heat of a superconducting spherical sample of 7.05 wt% Pb–In alloy in constant applied magnetic fields at temperatures between 1.6 and 4°K has been measured. The alloy was prepared by the Indium Corporation of America from 99.999% pure indium and 99.999% pure lead. A sphere of 2-in. diam was obtained by vacuum-casting the material into a spherical graphite mold. After a 10-h cooldown the sample was annealed at 135°C for 10 days. A vacuum calorimeter with a mechanical heat switch was used in conjunction with carbon resistor thermometry.

The results are presented in Fig. 1 as $[c(H_0,T)-c_n(T)]/T$ versus T, in which H_0 is the applied field and c_n is the specific heat in the normal state. The field was always applied after the sample had been cooled down to the lowest temperatures.

The value of the normal specific heat at temperatures below 2.5°K could be fitted to $c_n=1.75T+1.704T^3$ (mJ/mole °K) with a standard deviation of 0.5%. The coefficient of the electronic term $\gamma=1.75$ mJ/mole (°K)^2 is larger than the value of $\gamma=1.60$ mJ/mole (°K)^2 for pure In.[1] Ninth-order polynomials in odd powers of T were used to fit both c_n and c_s over the whole temperature range of the measurements. About 70 points were used for each fit, and the standard deviation was less than 0.6%. No systematic deviation of the measured points from the fits could be detected. The lattice specific heat $c_l=c_n-\gamma T$ [with $\gamma=1.75$ mJ/mole (°K)^2] was compared with the Debye expression and an effective temperature-dependent Debye temperature $\Theta_D(T)$ was determined. It has an approximately constant value of 104.5°K at temperatures below 2.5°K and then drops rapidly to 99.5° at 4°K.

The critical temperature was $T_c=3.65$°K. It is not inconsistent with the data to assume a zero-field transition width of less than 15 mdeg. Assuming zero transition width, the fits for c_n and c_s were used to calculate the thermodynamic critical field $H_c(T)$ from the re-

* Work supported by the U.S. Atomic Energy Commission and the Wisconsin Alumni Research Foundation.

[1] C. A. Bryant and P. H. Keesom, Phys. Rev. **123**, 491 (1961).